Sustainable Cities and Society 84 (2022) 104018

Contents lists available at ScienceDirect

Sustainable Cities and Society

journal homepage: www.elsevier.com/locate/scs

Study on the spatial-temporal pattern and evolution of surface urban heat island in 180 shrinking cities in China

Xiaoxue Peng [a], Yinying Zhou [a], Xianhao Fu [a], Junfeng Xu [a,b,*]

[a] Institute of Remote Sensing and Earth Sciences, College of Science, Hangzhou Normal University, Hangzhou 311121, China
[b] Zhejiang Provincial Key Laboratory of Urban Wetlands and Regional Change, Hangzhou 311121, China

ARTICLE INFO

Keywords:
Shrinking cities
Surface urban heat island
Spatial and temporal variation

ABSTRACT

Under the background of rapid urbanization, the urban heat island effect becomes more and more intense, which is common in many big cities. However, it is unclear whether this change will lead to a new turnaround in the mitigation of the urban heat island effect in shrinking cities with population loss. In this study, based on the MODIS product from 2001 to 2019, we analyzed the spatial and temporal patterns of surface urban heat island (SUHI) in 180 shrinking cities in China. The changes of SUHI at different scales in combination with latitude and climate zones were quantified. The results showed that SUHI intensity varied greatly in different latitudes and climate zones. In the arid zone, the SUHI intensity is the lowest in the daytime and the highest in the night. Combined with the SUHI characteristics of typical expanding cities, SUHI of shrinking cities in China shows a decreasing trend. This indicates that in shrinking cities, the decrease of population has a certain easing effect on SUHI. However, the driving mechanism behind it needs to be further explored so as to put forward specific measures to alleviate SUHI more specifically.

1. Introduction

Over the past few decades, the world has experienced a rapid process of urbanization. Against the background of explosive growth of urban population in general, some cities are currently facing shrinkage characterized by population loss due to changes in industrial structure (He et al., 2017), aging population (Döringer et al., 2020), suburbanization (Wiechmann & Pallagst, 2012) and other problems, which are called shrinking cities. For example, Leipzig in Germany (Martinez-Fernandez et al., 2016), Detroit in the United States (Danko & Hanink, 2018) and Northeast China (Yang et al., 2021). At present, there is no unified definition for shrinking cities, but the academic community generally regards population reduction as an important criterion to judge whether cities shrink or not (Gao, 2015). According to the Shrinking Cities International Research Network (SCIRN), three conditions need to be met for a shrinking city: urban areas with a population of 10,000 or more, most areas experiencing at least two years of depopulation, and accompanied by structural economic transformation and crisis (Wiechmann, 2008). With population loss, urban development and residents' production and life in shrinking cities have undergone obvious changes: insufficient economic development motivation (Liu et al., 2019), reduced social vitality level (Murdoch, 2018), increased number of vacant houses (Gu et al., 2019), uneven quality of public space (Schetke & Haase, 2008), etc. On the other hand, the decrease of population can relieve the pressure on environment and resources to some extent. Taking surface thermal environment as an example, population loss will weaken industrial production intensity, reduce road traffic flow, and reduce residents' living energy consumption. This results in a significant reduction in anthropogenic heat emissions in the city, thus improving the surface thermal environment. Furthermore, the spatial distribution of surface heat pattern is consistent with the degree of population loss. In addition, the reduction of human disturbance and optimization of ecological conditions also provide the possibility to alleviate the surface urban heat island (SUHI) effect. At present, global warming continues and extreme weather phenomena occur frequently. Therefore, studying the SUHI mitigation trend of shrinking cities can not only provide new ideas for human adaptation and mitigation of climate change in the future, but also have important practical significance for regulating regional climate and improving the global surface thermal environment.

Urban heat island (UHI) effect refers to the phenomenon that the temperature of a city is higher than that of the surrounding suburbs due to human activities. It is one of the most important ways that human

* Corresponding author at: Institute of Remote Sensing and Earth Sciences, College of Science, Hangzhou Normal University, Hangzhou 311121, China.
E-mail address: 20090019@hznu.edu.cn (J. Xu).

https://doi.org/10.1016/j.scs.2022.104018
Received 8 March 2022; Received in revised form 28 May 2022; Accepted 20 June 2022
Available online 21 June 2022

beings change the earth. The UHI can generally be grouped into three types, namely subsurface UHI (SubUHI), surface UHI (SUHI), and canopy layer UHI (CLUHI) (Pichierri et al., 2012; Zhan et al., 2014; Zhou et al., 2019). SUHI is defined based on the land surface temperature measured by satellite, which has significant advantages over traditional surface measurement methods such as wide coverage and high timeliness (Venter Zander, Chakraborty, & Lee, 2021). Some studies have quantified the spatial and temporal pattern of global urban SUHI and analyzed its evolution characteristics (Chakraborty & Lee, 2019; Peng et al., 2012). They calculated SUHII at different time scales and spatial partitions mainly by using MODIS data of long time series. The assessment included diurnal, monthly, seasonal and annual characteristics of SUHII, as well as SUHII differences between different latitude and climate zones. The relationship between various driving factors and SUHI intensity was further analyzed. Anthropogenic heat emissions, for example, have been shown to correlate significantly with the distribution of SUHII both during the day and at night (Zhou et al., 2014). Multi-city-oriented researches can reveal SUHI characteristics with certain value. However, once choosing subjects only based on geography (such as a city cluster, a country or even the world), it is possible to draw similar conclusions from many seemingly different experiments, which is of little significance.

The SUHI character of shrinking cities remains largely unknown. Most previous studies focus on one or several specific cities. Due to the differences of study areas, shrinking cities in different regions show different patterns of SUHI effect. Rohinton and Eduardo explored the climate change characteristics of Glasgow, a shrinking city in The United Kingdom (Emmanuel & Krüger, 2012). They used the measured data of meteorological stations, and found that although the population of the city continued to decline in the past 50 years, regional warming still existed. The basic urban form remained almost unchanged, leading to the continuation of abnormal climate. Different from Glasgow, the SUHI intensity of Hegang and Dongguan in China shows a slowing trend as a whole during the period of population contraction. In addition to population factors, a series of measures such as building land control and eco-city development also play a certain role (Hou, 2020). The research on an individual city can describe the characteristics of regional SUHI in detail, but cannot reflect the trend of SUHI evolution with population loss of shrinking cities as a whole. In addition, it has not been confirmed whether the conclusion obtained by only studying the shrinking cities really represents the increase or decrease of their SUHI. It is necessary to further compare the expanding cities to obtain the common trend of shrinking cities development SUHI from the macro level.

In this study, we use land surface temperature and land cover datasets from the Mid-Resolution Imaging Spectroradiometer (MODIS) from 2001 to 2019 to determine surface urban heat island intensity (SUHII) for 180 shrinking cities in China. The main objective is to explore whether SUHI in shrinking cities shows a certain trend of remission under the background of population loss. The spatial and temporal patterns of SUHI in shrinking cities are quantified, and the long-term evolution characteristics of SUHI are analyzed in combination with latitude and climate zones. In order to understand the real development trend of SUHI in shrinking cities, a comparative study is conducted on typical expanding cities. This is also an innovation of this study. Does population reduction change the original SUHI trajectories of cities by reducing anthropogenic heat emissions? Do the two cities with opposite population flow patterns also show opposites in the changing trend of SUHI? The results of these problems are of great significance for grasping and predicting the environmental development of shrinking cities and putting forward more practical measures to alleviate the SUHI effect and improve urban ecology.

2. Data and methods

2.1. Area

We select 180 shrinking cities in China to study the spatio-temporal distribution and variation characteristics of SUHI from 2001 to 2019 (Fig. 1). Based on the data of the fifth and sixth population censuses at the township and street level in China, 180 cities of 654 cities at the county level and above were identified to have a declining population/density (Long et al., 2015). The shrinking cities in China are characterized by large number and wide distribution: among 180 cities, there are 1 provincial capital city, 39 prefecture-level cities and 140 county-level cities, covering 25 provinces. Geographically, shrinking cities are distributed throughout China. Among them, central China (45), East China (44) and northeast China (34) have relatively large numbers, accounting for about 70% of the total number of shrinking cities in China. When defining the city scope, we clearly distinguish prefecture-level cities and county-level cities. Cities at prefecture-level and above adopt the scope of their municipal districts in 2012, while county-level cities adopt the scope of their administrative regions in 2012.

2.2. Datasets

Data used in the study include land surface temperature, land cover and global climate subregions. Data processing is performed on the Google Earth Engine (GEE) platform. Earth Engine is an online platform for processing remote sensing images launched by Google in 2011, supporting scientific analysis and visualization of geospatial data sets. It contains massive basic data and can be easily called, so it is suitable for processing long time series and large range remote sensing images.

2.2.1. Land surface temperature

Land surface temperature (LST) data are derived from MODIS daily Land Surface Temperature synthesis products MOD11A1 and MYD11A1 (version 6), with 1km spatial resolution, provided by NASA. LST is obtained by inversion of thermal infrared bands 31 and 32 using split window algorithm, and the accuracy is better than 1K (Wan et al., 2015). MOD11A1 used in this paper is acquired by the Terra satellite and recorded LST of 1030 LT and 2230 LT, covering the years 2001-2019 (6, 893 images in total). MYD11A1 is acquired by the Aqua satellite and recorded LST at 0130 LT and 1330 LT. Because the dataset is available since 2002, the year range is from 2003 to 2019 (6,207 images).

2.2.2. Land cover type

Land cover type data are derived from MCD12Q1 (version 6), a level 3 land cover type product of MODIS Terra and Aqua, with a spatial resolution of 500m × 500m. The product uses six different classification schemes to monitor and classify the reflectance data of two MODIS sensors. After post-classification processing, specific categories are further refined by combining prior knowledge and auxiliary information, and annual global land cover type information is obtained (2001-2019). It has been verified that the classification results of the International Geosphere-Biosphere Programme (IGBP) in this product have an estimated accuracy of 73.6% worldwide (Friedl & Sulla-Menashe, 2019). IGBP classification is composed of 17 main land cover types, including 11 natural vegetation types, 3 land use and Mosaic types and 3 non-vegetation land types, which has relatively rich data types. Therefore, based on the results of IGBP classification, this study extracted the urban areas of shrinking cities in China from 2001 to 2019.

2.2.3. Köppen-Geiger climate classification

Köppen-Geiger climate classification divides the world into 5 basic climate zones and 12 main climate types based on vegetation type, temperature and precipitation. It is one of the mainstream climate classification methods with the most extensive application and the

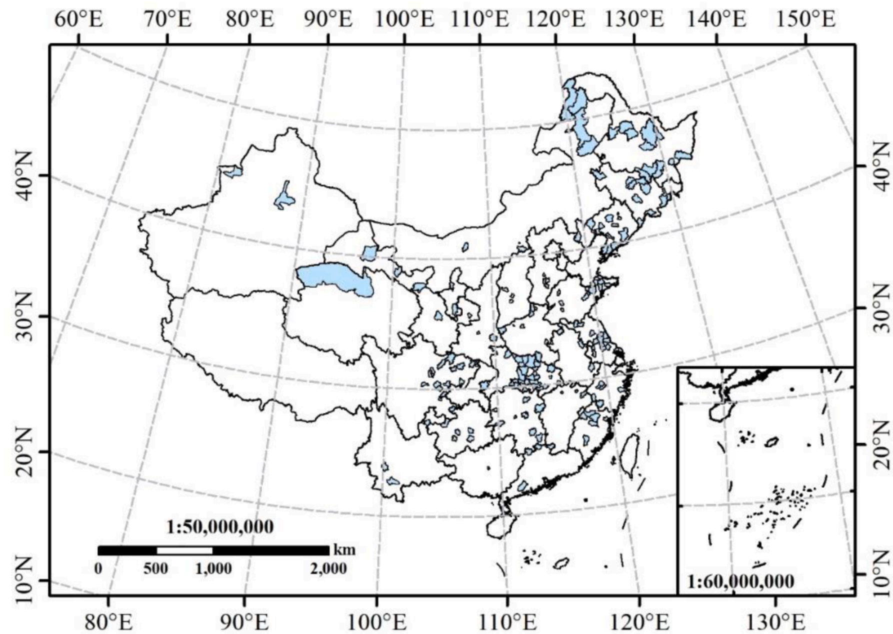

Fig. 1. Distribution of shrinking cities in China.

greatest influence in the world (Zhu & Li, 2015). We download the updated KMZ data of Köppen-Geiger climate classification world map from the website (http://koeppen-geiger.vu-wien.ac.at/) from 1986 to 2010, and combine with the city area vector data of shrinking cities to divide the climate zones of each city. The results show that the 180 shrinking cities in China mainly involve the basic climate zones including arid, warm temperate and snow. The main climate types are cold semi-arid climate (BSk), cold desert climate (Bwk), humid subtropical climate (Cwa, Cfa), subtropical oceanic highland climate (Cwb), humid continental climate (Dwa, Dwb) and cool continental climate (Dwc). The distribution and number of shrinking cities in each climate zone are shown in Fig. 2 and Table 1 respectively. The number of

Table 1
Number of shrinking cities in each climate zone.

Climate zone	Climate type	Number	Total
Arid (B)	Cold semi-arid climate (BSk)	17	24
	Cold desert climate (Bwk)	7	
Warm temperate (C)	Humid subtropical climate (Cfa)	71	117
	Humid subtropical climate (Cwa)	43	
	Subtropical oceanic highland climate (Cwb)	3	
Snow (D)	Humid continental climate (Dwa)	18	39
	Humid continental climate (Dwb)	18	
	Cool continental climate (Dwc)	3	

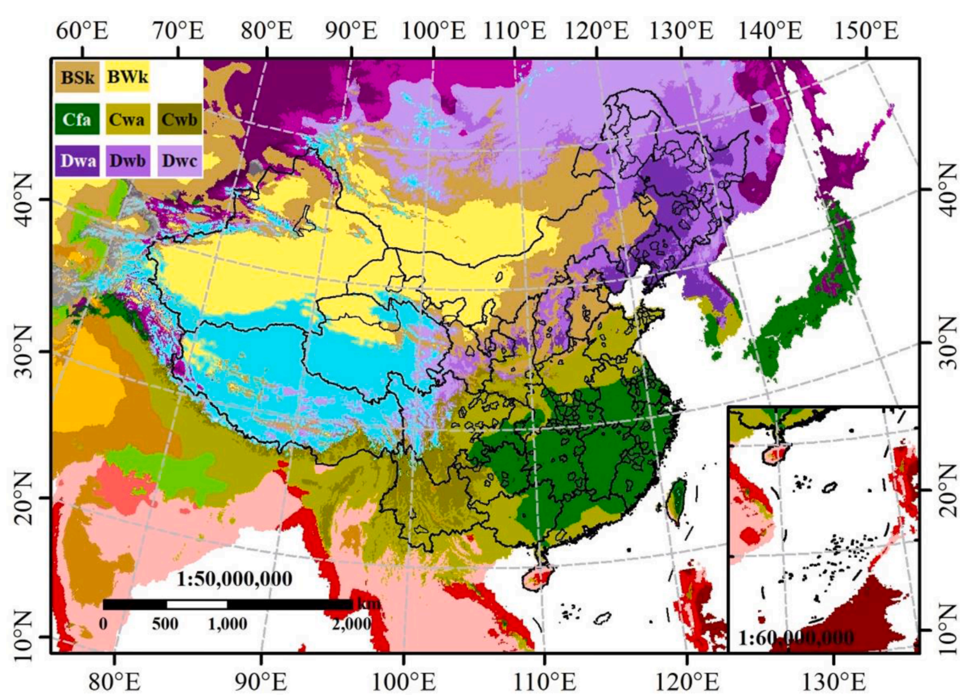

Fig. 2. Distribution of shrinking cities in each climate zone.

shrinking cities in warm temperate climate zone is the largest, and most of them are in humid subtropical climate.

2.3. Surface urban heat island intensity calculation

There are two main methods to extract SUHI, depending on whether to divide urban areas and suburbs. One is to consider the relationship between the city and its surrounding environment. And the commonly used methods include mean-standard deviation method (Qiao & Tian, 2014), equidistance method (Chen & Wang, 2009), heat island intensity calculation method (Pan et al., 2020), etc. The other is to define SUHI as the LST difference between urban and suburban areas on the basis of clearly defining the scope of two. According to different suburban pixel selection strategies, they are reference pixel method and buffer method

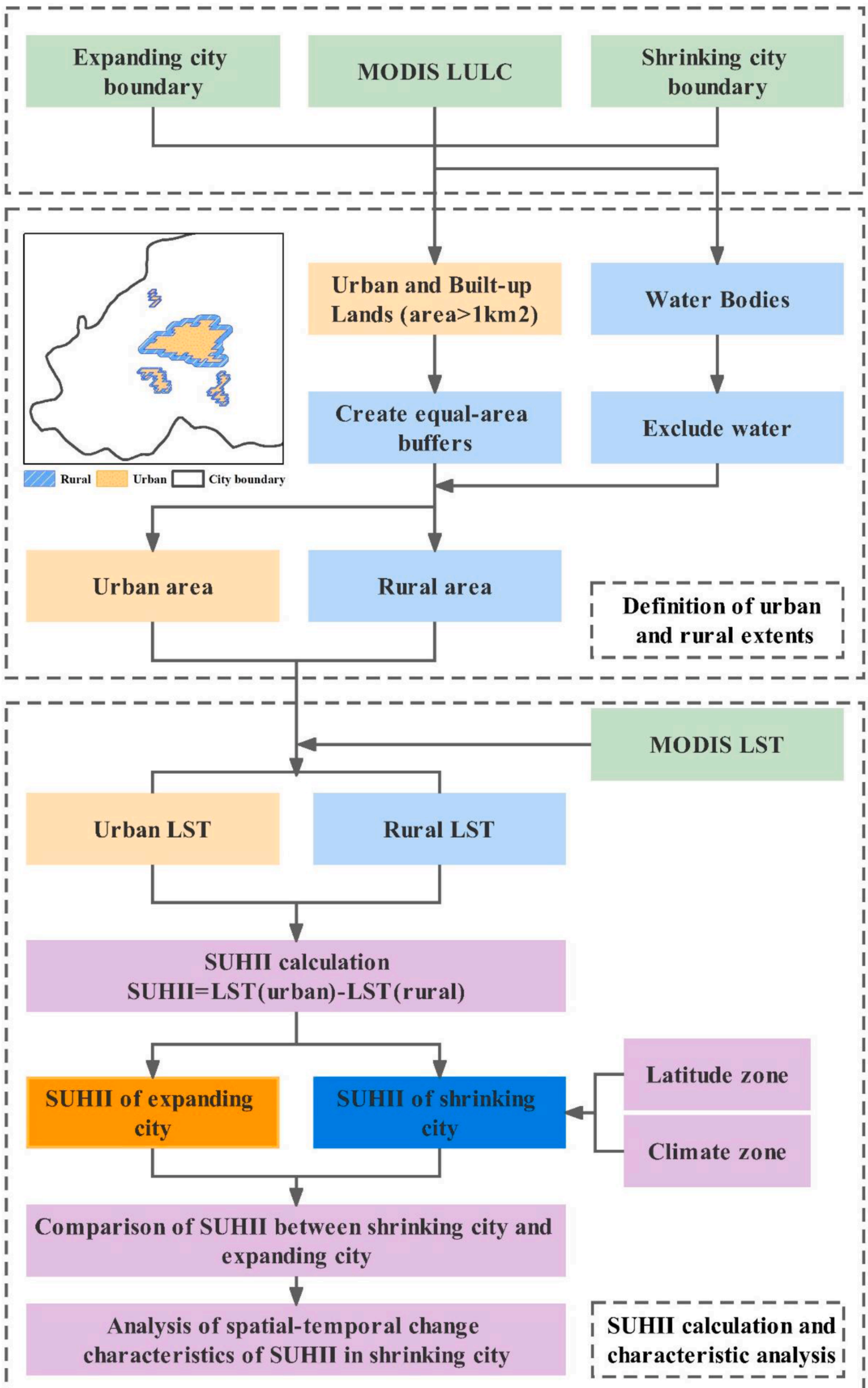

Fig. 3. Workflow of the study.

(Sun et al., 2021). Among them, buffer method defines suburban area by setting equidistant buffer zone (such as radius 20km (Yao et al., 2017)) or selecting peripheral buffer zone equal to corresponding urban area (Sun et al., 2019) on the premise of city scope being known, and calculates suburban temperature difference as UHI intensity value.

In this study, the equal area buffer method is used to estimate the SUHII of shrinking cities in China. This method avoids the subjectivity of reference pixel selection and is convenient for comparison between different cities. Fig. 3 shows the overall workflow of the study. We extract urban and construction land categories under IGBP classification from MCD12Q1 as urban areas. And to the city as the core to do equal area of the buffer zone as the surrounding suburbs. The SUHII of each city is calculated by the difference between the average surface temperature of the urban area and its suburb. In order not to hide the slight differences of urban boundaries between different years, urban areas are extracted from 2001 to 2019 year by year. And only urban agglomerations larger than $1km^2$ are retained to match the resolution of MODIS LST data. Because the high specific heat capacity of water will lead to overestimation of daytime UHI intensity and underestimation of nighttime UHI intensity, water pixels in urban areas and suburbs need to be removed (Chakraborty & Lee, 2019; Imhoff et al., 2010; Zhou et al., 2015).

3. Results

3.1. Temporal trends of SUHI in shrinking cities

3.1.1. Latitude characteristics

The shrinking cities are divided into latitude zones to analyze the impact of latitude factors on SUHII. The Chinese shrinking cities are mainly distributed between 20 ° and 55° north latitude. We divide the latitude in increments of 5° and classify each shrinking city into the corresponding latitude belt. When a city occupies two latitude zones at the same time, it is judged by the city area in each latitude zone. The latitude zone that captures most of the city area is what we are looking for. The number of shrinking cities contained in each latitude zone is shown in Table 2. All latitude zones contain relatively large numbers of cities, except for the smaller distribution of shrinking cities within the 20° -25° and 50° -55° north latitude zone. Most shrinking cities are located in the range of 30° -35° N.

The SUHII of each latitude zone is obtained by calculating the mean SUHII of all shrinking cities in the corresponding zone. Fig. 4 shows the variation of daytime and nighttime SUHII with latitude for shrinking cities from 2001 to 2019, derived from the combined results of Terra and Aqua. The daytime and nighttime SUHI of shrinking cities shows different patterns. Daytime SUHII is most significant in the range of 20°–25° N, while relatively weak in the range of 35°–40°N. The highest and lowest values of SUHII are 0.70°C and 0.16°C, respectively. The maximum nighttime SUHII appears in the range of 40°-45°N, about 0.44°C, and the lowest value existed in the band of 50°–55°N, about 0.21°C. With the increase of latitude, daytime SUHII weakens first and then slowly strengthens, while nighttime SUHII rises first and then falls. SUHII is higher during the day than at night in the range below 35°N and 50°–55°N.

Table 2
The number of shrinking cities across all latitude zones.

Latitude zone (N)	Total
20°–25°	5
25°–30°	39
30°–35°	63
35°–40°	31
40°–45°	28
45°–50°	12
50°–55°	2

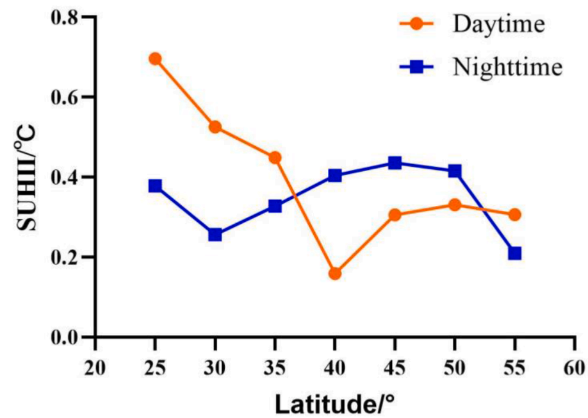

Fig. 4. Variation of SUHII with latitude in shrinking cities.

3.1.2. Climate zones characteristics

From 2001 to 2019, shrinking cities in different climate zones exhibit different daytime and nighttime SUHI characteristics. Fig. (a) and (b) in Fig. 5 show daytime and nighttime SUHII for each climate zone derived from Terra and Aqua, respectively. The maximum Terra daytime SUHII occurs in the warm temperate zone, followed by the snow zone and the arid zone. And nighttime SUHII is the highest in the arid zone, and there is little difference between warm temperate and snow zones. Aqua SUHII also exhibits similar characteristics to Terra SUHII during the day and night.

180 shrinking cities in China account for eight of the 12 main climate types in Köppen-Geiger climate classification, including BSk, BWk, Cfa, Cwa, Cwb, Dwa, Dwb and Dwc. Fig. 6 shows the daytime and nighttime SUHII of shrinking cities for eight major climate types. Both Terra and Aqua results show the highest SUHII for Cfa during the day, BSk and Dwa at night, and the lowest SUHII for BWk during the day and Dwc at night. For all climate types except Cfa, Dwb, and Dwc, Terra daytime SUHII is lower than nighttime. For Aqua, only BSk, BWk and Dwa SUHII are lower during the day than at night.

3.1.3. Long-term series characteristics

The long-term sequence change analysis results of daytime and nighttime SUHII in shrinking cities are shown in Fig. 7. Both daytime and nighttime SUHII have periodic variation laws, and the characteristics of daytime are more significant. High daytime SUHII values usually occur in the middle and late part of each year (roughly from June to September), while SUHII is relatively low at the beginning and end of the year. The fluctuation range of SUHII is larger in the daytime, with the difference between the highest and lowest values up to about 1.2°C, while only about 0.4°C at night. The results of linear fitting further indicate that the evolution trends of SUHII during daytime and nighttime are not consistent over the past two decades. The SUHI effect weakens in the daytime and strengthens at night. From the slope, SUHII trend is more obvious at night. Mann-Kendall non-parametric statistical test was used to analyze the trend and significance of long-term series SUHII in shrinking cities. *P* values were all less than 0.01, indicating that the trend was significant and had statistical significance.

The annual mean of SUHII for each climate zone from 2001 to 2019 is calculated. Fig. 8 shows the interannual variation of SUHII in shrinking cities in China from 2001 to 2019. Data from Terra and Aqua are calculated respectively, and the SUHII for each year is the annual mean SUHII for all shrinking cities in each climate zone. The dotted line in the figure shows the linear trend of SUHII over a 19-year period. The results from Terra and Aqua are similar. Except for the warm temperate zone, the daytime SUHI in other climate zones shows a weakening trend in the corresponding years. Especially, the decrease trend of SUHII is most significant in the arid zone. Nighttime SUHII increases year by year in all climate zones. For both Terra and Aqua, nighttime SUHII increases

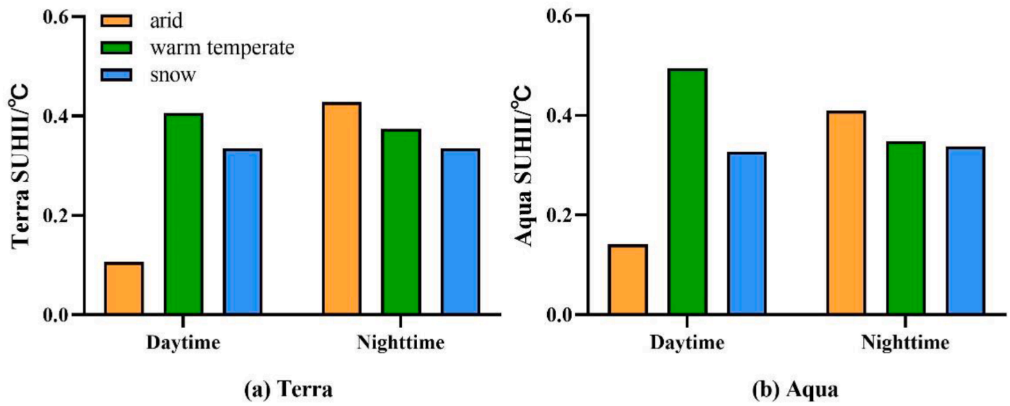

Fig. 5. Daytime and nighttime SUHII of shrinking cities in each climate zones.

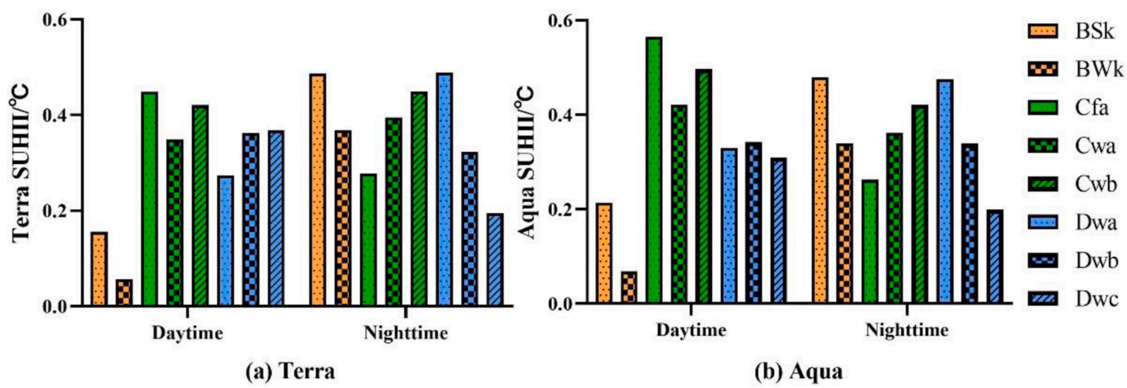

Fig. 6. Daytime and nighttime SUHII of shrinking cities for different climate types.

the most in the arid zone over the past 20 years. In general, the SUHI of shrinking cities shows different evolution characteristics from 2001 to 2019. It is weaker in the daytime and stronger at night, and the strengthening feature at night is more obvious. The results of significance test show that SUHII trend is significant in all cases only in the arid zone ($p< 0.01$). The SUHII trend of all shrinking cities is not significant during the daytime obtained by Terra.

3.2. Spatial pattern and evolution of SUHI in shrinking cities

To explore the spatial distribution and evolution characteristics of SUHI in shrinking cities of China from 2001 to 2019, the daytime and nighttime SUHII averages from Terra and Aqua for 2001 (or 2003) and 2019 of each shrinking city are calculated. The results are shown in Fig. 9. SUHII is graded in 0.5°C increments, including no SUHI effect (SUHII<0°C), relatively mild (0°C<SUHII<0.5°C), moderate (0.5°C<SUHII<1°C) and severe SUHI effect (SUHII>1°C). Daytime and nighttime SUHII of most cities are in the range of 0-1°C, and cities with moderate and severe SUHI effect are distributed in central, southern and northern China. For Terra and Aqua, the daytime SUHI effect is more significant in the south-central region, and the distribution of high SUHII is more concentrated. Nighttime SUHI effect is relatively scattered in central and northern China.

Results extracted from Terra show that high daytime SUHII is mainly located in the south-central region in both 2001 and 2019. By contrast, cities of moderate SUHI are more dispersed in 2001 and tended to cluster southward in 2019. The number of cities with severe SUHI has increased. For example, Chibi in central and south China, Qionglai, Lincang and Pu 'er in southwest China have changed from moderate or mild SUHI to severe SUHI. The number of cities with no or mild SUHI in central and northern China also increased, and the SUHI effect is strong in the south and weak in the north. Nighttime SUHI did not show obvious spatial migration characteristics during the past 20 years. However, in 2019, a large number of cities change from mild to moderate SUHI within the concentrated distribution range of cities that originally showed moderate SUHI. For example, Feicheng, Yucheng, Jizhou, Xinyang, Pizhou, indicating that nighttime SUHI effect has been strengthened.

The results from Aqua and Terra are similar to some extent. In the daytime, the shrinking cities with severe SUHI in 2019 have diffusion characteristics compared with 2003. For example, Lanxi, Longquan, Jiangyou and Qionglai change from mild and moderate SUHI to severe SUHI. At the same time, the number of cities without SUHI in the north also increases, showing a zonal distribution in space. In addition to the increase in the number of cities with moderate SUHI at night, some cities with no SUHI show mild SUHI in 2019, such as Lanxi, Yuanjiang, Yicheng and Chishui. The results from both Terra and Aqua show that from 2001 to 2019, the daytime SUHI effect of shrinking cities weaken, while the nighttime SUHI increase.

4. Discussion

4.1. Temporal variation of SUHI in shrinking cities

This study mainly refers to Chakraborty et al. 's research on global scale extraction of SUHI and its spatiotemporal change analysis (Chakraborty & Lee, 2019). The temporal variation characteristics of SUHI in shrinking cities are analyzed from three perspectives: latitude zone, climate zone and all shrinking cities. Different from similar global SUHI studies, this study focuses on the characteristics of SUHI in cities with population loss and tries to reveal the potential effect of population reduction on SUHI mitigation. That's the innovation of the work. For the

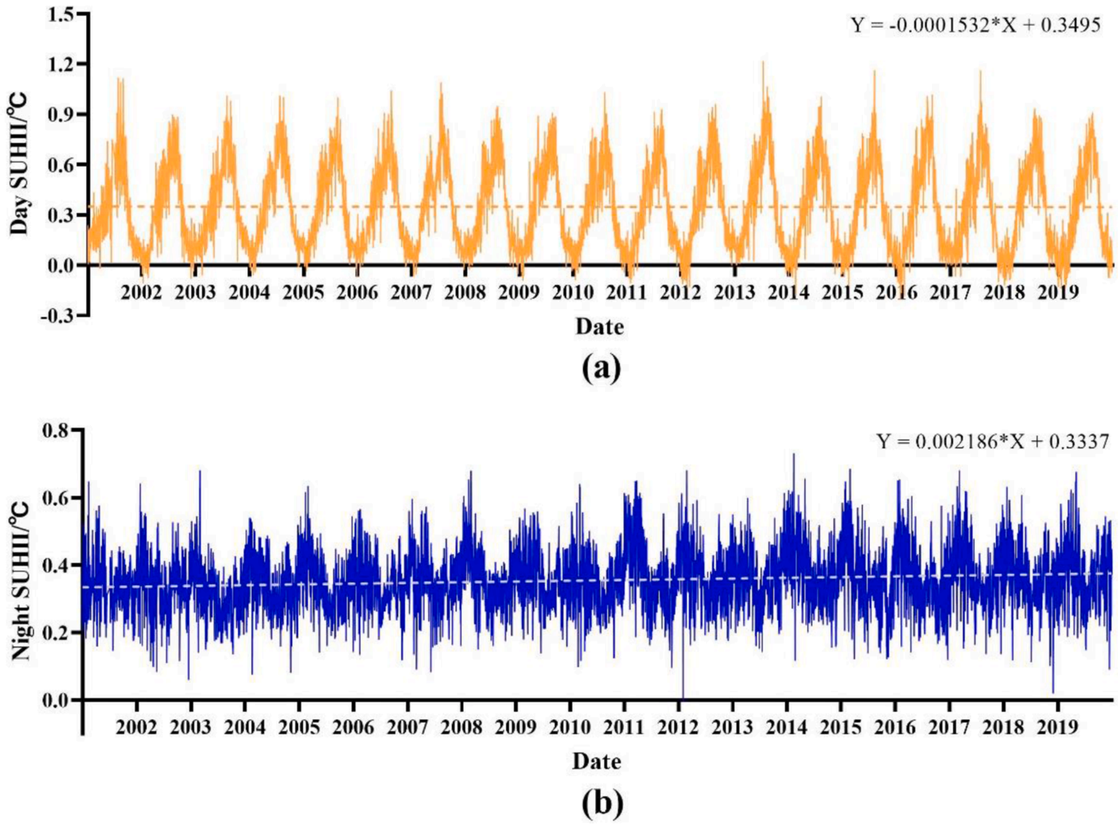

Fig. 7. Long-term changes of daytime and nighttime SUHII in shrinking cities. Fig. (a) and (b) correspond to daytime and nighttime SUHII, respectively, and are the combined results of Terra and Aqua.

first time, the SUHI results of shrinking and expanding cities were compared to obtain the real evolution trend of SUHI in shrinking cities. The results are of great significance to enrich the mitigation measures of SUHI, and can also provide some inspiration for the development of similar studies in the future.

The diurnal and monthly characteristics of SUHI in shrinking cities are generally consistent with some existing global results (Peng et al., 2012), so it is not presented here as a special conclusion. For shrinking cities, SUHII at night is higher than daytime SUHII at relatively high latitudes. Within the same latitude range (20°-55° N), global cities show this characteristic at lower latitudes. The reason for this phenomenon is that the shrinking cities in the high latitude zone of China belong to the arid zone, and nighttime SUHII is the highest in the arid zone according to this research. SUHII of the warm temperate zone in shrinking cities is higher than that of the snow zone, which is contrary to the global rule. The shrinking cities in the snow zone are mainly located in the northeast of China, while cities in the warm temperate zone are widely distributed in the central, eastern and southern of China. The distribution of population in China is characterized by more in the southeast and less in the northwest. So, in the warm temperate zone, the population of cities is generally higher than that in the snow zone, which may bring more anthropogenic heat emission. The long time series changes of SUHI in shrinking cities show a significant decreasing trend in daytime, suggesting that SUHI might be alleviated by population reduction. But this is not reflected in long-term changes in global SUHI.

4.2. Variation trend of SUHI in shrinking cities

On the basis of obtaining the overall changes of SUHII in all shrinking cities, the study further carries out trend analysis of daytime and nighttime SUHII of each shrinking city, and counts the number of shrinking cities under each linear trend (Table 3). According to the statistical results, 28 of the 180 cities show a linear decrease in daytime and nighttime SUHII extracted from Terra. The number of cities with a linear upward trend and the number of cities with an opposite linear trend is far more than this value, 54 cities and 98 cities respectively. The number of cities with declining trend, rising trend and opposite trend in daytime and nighttime SUHII obtained from Aqua is 23, 61 and 96, respectively. Only a few cities have seen the expected SUHI mitigation. The number of cities with the same variation trend in daytime and nighttime SUHII from Terra and Aqua is 10 (linear decrease) and 38 (linear increase), respectively. This may be due to the different year ranges of the two datasets, leading to trend changes. Or the land surface temperature recorded by sensors at different times is different, which makes the trend more uncertain.

The 10 cities with decreasing SUHII obtained from Terra and Aqua are Erguna, Yumen, Jian 'ou, Lechang, Mishan, Mianzhu, Pengzhou, Urumqi, Yichun (municipal district) and Hegang (municipal district). The severe shrinkage phenomenon is mainly concentrated in northeast China (Zhang et al., 2020). The northeastern cities involved in this study include Mishan, Yichun and Hegang. Among them, Yichun and Hegang are typical shrinking cities. Their overall change trend of SUHII is shown in Fig. 10. The results of significance test show that SUHII decreased significantly at night in the two cities, but not in the daytime. The SUHII of Yichun and Hegang recorded by Terra and Aqua were generally weak in the past 20 years, neither of which exceeded 1.5°C. SUHII of all shrinking cities shows significant volatility between 2001 and 2019. This indicates that there are complex influencing mechanisms behind the SUHI effect.

As one of the representative cities of resource exhaustion, Hegang is taken as an example (Sun & Li, 2013). On the one hand, with the vigorous exploitation of resources, coal and other resources are gradually exhausted. The traditional pillar industries cannot support the economic development of cities, so the population has to choose to flow

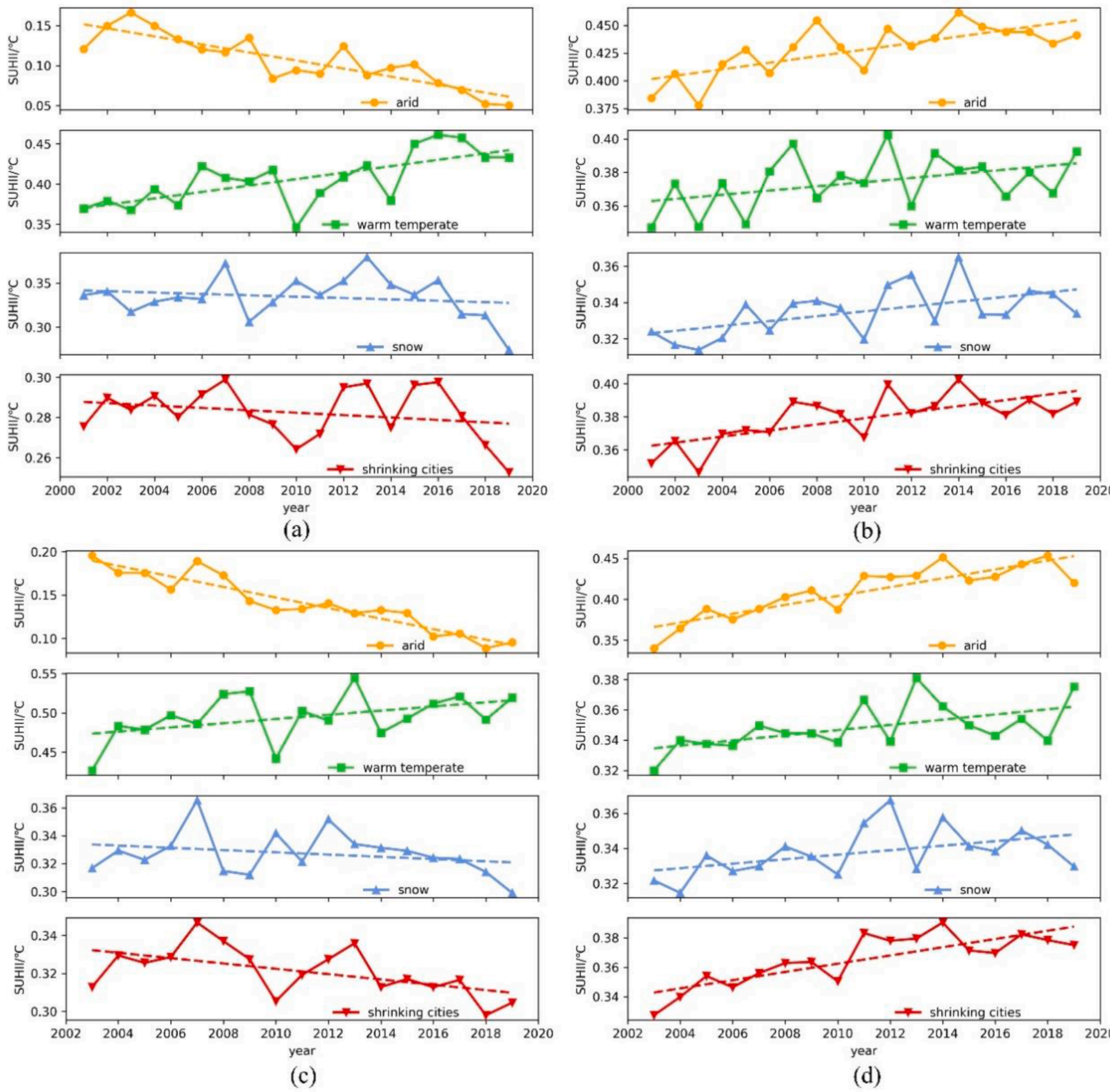

Fig. 8. Annual mean values of daytime and nighttime SUHII of shrinking cities in each climate zone. Fig. (a) and (b) show the daytime and nighttime SUHII from Terra. Fig. (c) and (d) correspond to the daytime and nighttime SUHII from Aqua.

to other cities to find new development opportunities. On the other hand, the depletion of resources forces cities to embark on the road of economic transformation. In the process of industrial restructuring, a number of enterprises will go bankrupt, resulting in a large number of laid-off workers, and further accelerate the outflow of population (Zeng & Duan, 2018). In this context, the number of enterprises with high energy consumption is reduced and the population is lost. The emission of industrial heat and anthropogenic heat in cities also decreases to a certain extent, making the SUHI effect relatively alleviated. In addition, the decrease of SUHII in Hegang may be related to the transformation of tourism and urban ecological construction. Hegang mainly relies on the border river tourism, developing tourism and improving the ecological environment go hand in hand. Nowadays, Hegang has achieved remarkable achievements in governance. By 2019, 10,500 mu of forest has been planted, the urban forest coverage rate has reached 70.4%, and the per capita park green area is 15m^2 (Wang, 2020). Since the cooling effect of vegetation and the role of mitigating the SUHI effect have been reached consensus in academic circles, the increase of green space area can provide a reasonable explanation for the decrease of SUHII in Hegang.

4.3. Comparison of SUHI between shrinking cities and expanding cities

During nearly two decades of population contraction, daytime and nighttime SUHII in 180 Chinese shrinking cities shows different development patterns (Figs. 7 and 8). During the day, results from both Terra and Aqua show a moderating SUHI effect, while SUHII increases significantly at night. Therefore, it is difficult to determine whether the SUHI effect is increasing or decreasing with population loss only from the evolution trend of SUHII in shrinking cities. In fact, population outflow and inflow usually happen together. This means that some cities are shrinking, and some of the more advanced metropolises are siphoning off the population of their smaller neighbors, leaving them facing rapid population expansion. We call these cities "sprawl cities."

Population size (Cheng et al., 2016) and density (Zhu et al., 2010) are closely related to SUHI, which will theoretically lead to different evolution results of SUHI effect in shrinking cities and expanding cities. To verify this phenomenon, we select some typical expanding cities to explore the development trend of the SUHI effect, including Beijing, Shanghai, Guangzhou, Shenzhen and Chengdu. Traditional first-tier cities in China, namely Beijing, Shanghai, Guangzhou and Shenzhen, have always been hugely attractive to the population. According to census data released by the National Bureau of Statistics (http://www.

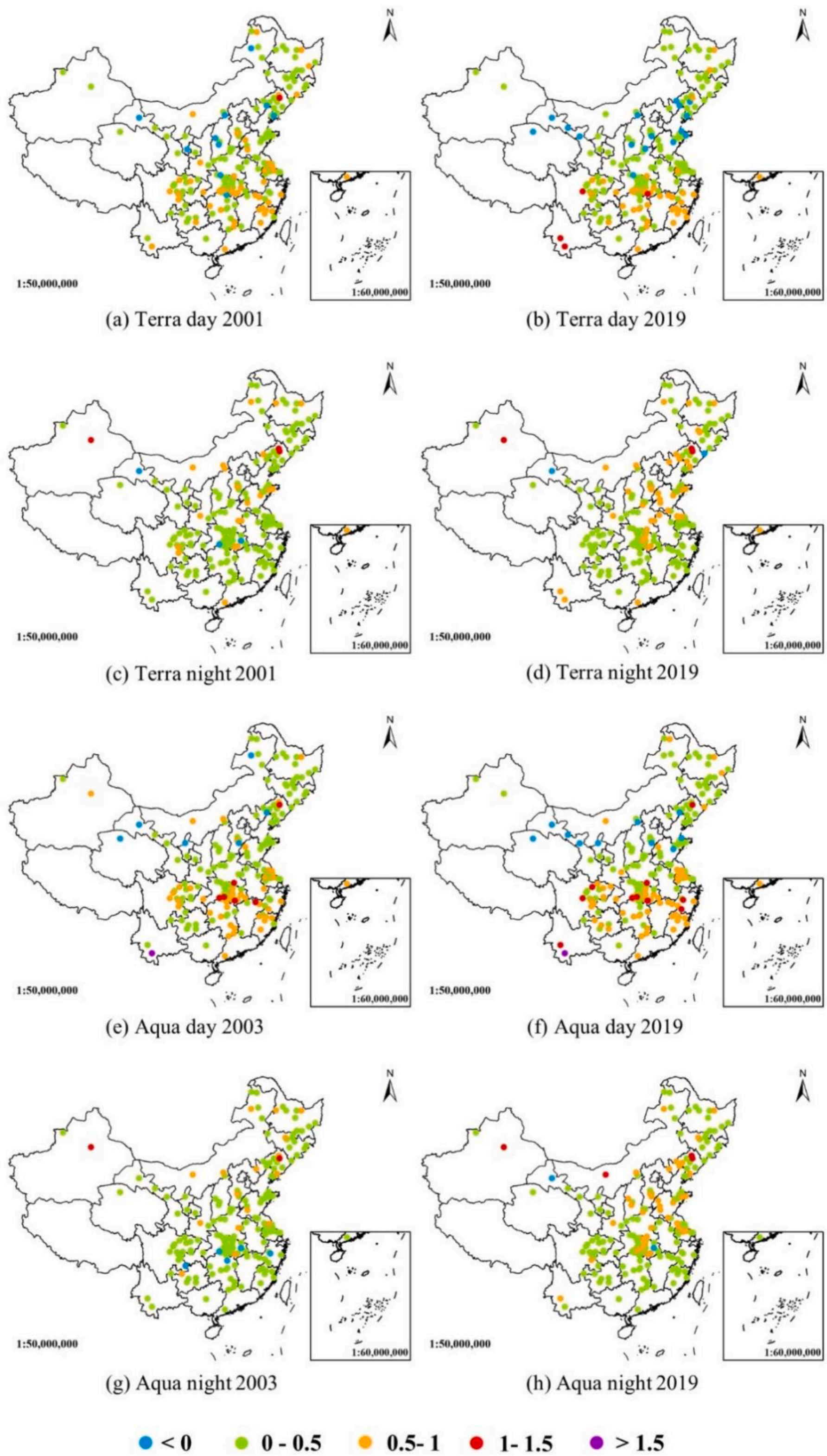

Fig. 9. The annual mean values of daytime and nighttime SUHII in shrinking cities. Fig. (a)–(d) show the daytime and nighttime results from Terra in 2001 and 2010 respectively. Fig. (e), (f) correspond to the daytime and nighttime results from Aqua in 2003 and 2010 respectively.

stats.gov.cn/), the number of permanent residents in these cities has continued to increase over the past two decades. In addition, four first-tier cities rank among the top four in China in the latest net inflow of population, based on the seventh census data. As a rising star, Chengdu has attracted a large population inflow in the past decade with its active new economy industries and loose talent policy. The population growth rate of Chengdu is obvious, and the net inflow of population ranks sixth in China.

Using the same SUHII calculation method as the shrinking city, the long-term change characteristics of SUHII in expanding cities are obtained (Fig. 11). Here SUHII is the combined result of the Terra and Aqua satellites. The results show that SUHI is significantly different between

Table 3
The number of shrinking cities under each linear trend of daytime and nighttime SUHII.

Satellite	Number of shrinking cities with a linear decrease in daytime and nighttime SUHII	Number of shrinking cities with a linear increase in daytime and nighttime SUHII	Number of shrinking cities with an opposite linear trend in daytime and nighttime SUHII
Terra	28	54	98
Aqua	23	61	96
Terra & Aqua	10	38	/

expanding cities and shrinking cities. The difference is first intuitively reflected in the value of SUHII. The daytime or nighttime SUHII in the expanding cities can reach or even exceed 1°C, and the daytime SUHII in Shenzhen exceeds 1.5°C. The SUHII of shrinking cities is generally low, and the annual mean is mostly distributed in the range of 0–0.5°C. Almost no shrinking cities have SUHII over 1.5°C. The SUHII trends of the two types of cities also show different characteristics over time. SUHII increases in both day and at night in the expanding cities, and most of the increasing trends are significant ($P < 0.05$). In the shrinking cities, SUHII is weakened during the day and strengthened at night. In addition, the SUHII of the expanding cities increases significantly, and the SUHII range of all the expanding cities exceeds 0.1°C. Among them, SUHII in Shenzhen increases the most in the daytime, reaching 0.68°C. SUHII increases the most in Beijing at night, with an increase of about 0.38°C. Compared with the change range of SUHII in expanding cities, the value of SUHII in shrinking cities increases less than 0.1°C at night (The difference between the highest and lowest values of SUHII is 0.05°C for Terra and 0.06°C for Aqua). Although shrinking cities show an upward trend of nighttime SUHII, the increase is slow and smaller than that of typical expanding cities. In conclusion, the SUHI effect of cities with shrinking population is considered to be alleviated in the selected year range.

4.4. Limitations and future perspectives

There are also several aspects that may be improved in future work. On the one hand, due to the lack of a unified definition of shrinking city, there are many kinds of shrinking city identification results in China (Long et al., 2015; Meng & Long, 2022; Wu, 2019). The study chose a more widely accepted identification of 180 shrinking cities in China. But the results, which use China's once-a-decade census data, do not actually reflect year-to-year population changes. At present, there is no public relatively authoritative annual population data of each city. Therefore, this study does not consider the dynamic change of population between years, and considers that all shrinking cities show a decrease in population as a whole. The identification of shrinking cities will be more accurate if we can obtain high-quality and long-term detailed population data in the future. In carrying out SUHI research, the method proposed in this paper can be used to more accurately reveal and explain the unique model of SUHI in shrinking cities by combining the dynamic changes of population in quantity and space. In addition, in order to verify the conclusion that SUHI alleviates with population loss, an excellent method is to carry out a comparative study of SUHI changes before and after city shrinkage based on the known start time of contraction. Such research can more intuitively show the impact of regional population flow on SUHI, but now it is difficult to implement due to lack of data. It should be noted that SUHI changes with population may have a lag, so data needs to be fully collected for years before and after the point in time of shrinkage. And that's also going to be a big challenge.

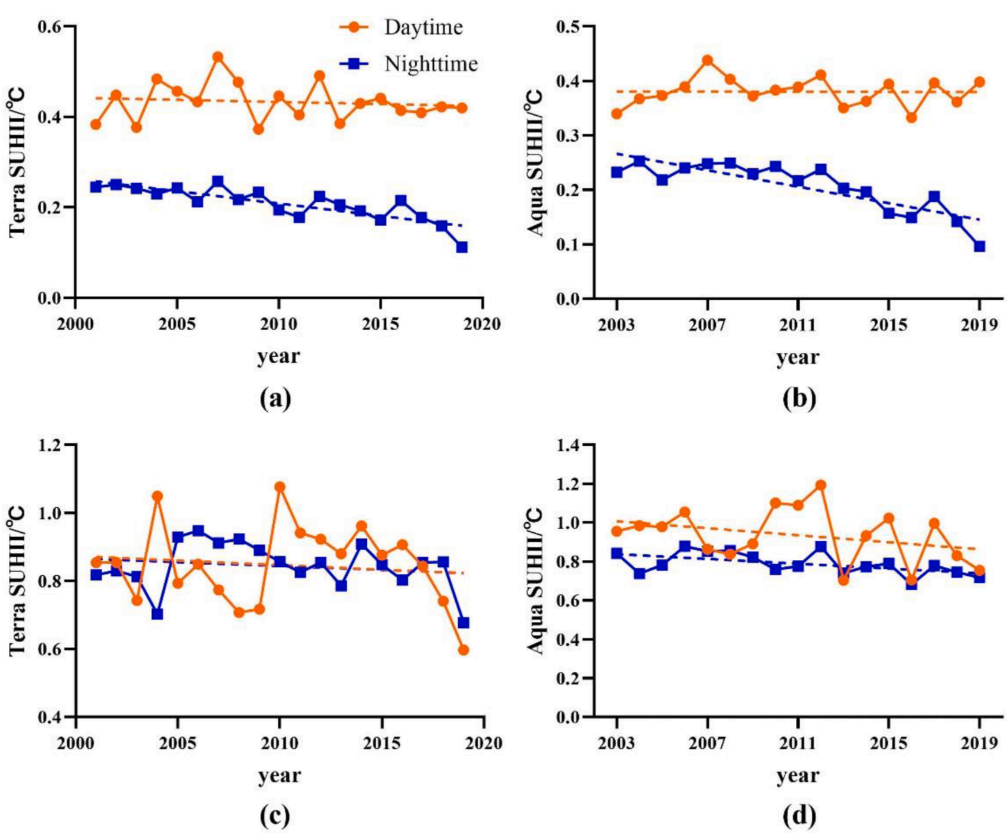

Fig. 10. Variation trend of SUHII in Yichun and Hegang. Fig. (a) and (b) show daytime and nighttime SUHII obtained by Terra and Aqua in Yichun. Fig. (c) and (d) show daytime and nighttime SUHII obtained by Terra and Aqua in Hegang.

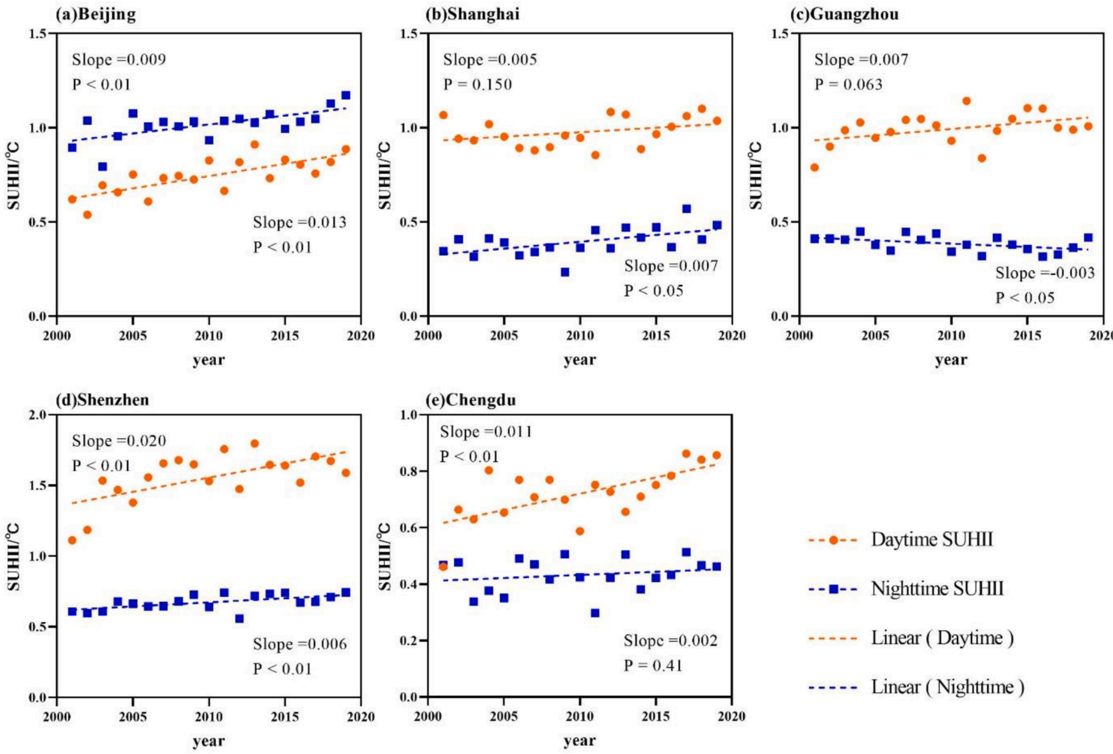

Fig. 11. Long-term trends of SUHII in the expanding cities. Fig. (a)–(e) respectively represent daytime and nighttime SUHII in Beijing, Shanghai, Guangzhou, Shenzhen and Chengdu.

5. Conclusions

In this study, we analyze the spatial and temporal patterns and evolution characteristics of SUHI in 180 shrinking cities in China, and explore the changing rules of SUHI under population loss combined with latitude and climate factors. By comparing with the SUHI of the expanding cities, the mitigation trend of the shrinking cities SUHI is revealed. The results suggest that from 2001 to 2019, the SUHI of shrinking cities in China has generally eased.

For shrinking cities located in different latitude zones, the SUHI is strongest in the range of 20°−25° N during the day, and significant in the range of 40°−45° N at night. Under the Köppen-Geiger climate classification, the SUHII of shrinking cities in arid climate zone has special characteristics. In all climate zones, results from both Terra and Aqua show the lowest daytime SUHII and the highest nighttime SUHII in arid.

The spatial distribution pattern and variation characteristics of daytime and nighttime SUHI in shrinking cities are different. Shrinking cities with moderate and severe SUHI are distributed in central, southern and northern China. During the day, the high value of SUHII gradually gathers in the south. Although there is no significant migration at night, SUHII changes from mild to moderate in many cities. The overall trend of SUHII varies from city to city. Some cities show obvious mitigation characteristics of SUHI effect, which is consistent with the current situation of population loss, and the increase of vegetation area is also an important influencing factor.

The long-term series results show that the SUHI of shrinking cities and expanding cities are significantly different. SUHII of shrinking cities decreases in the daytime and increases at night, while SUHII in typical expanding cities increases almost both day and night. Compared with the rapid increasing SUHI effect in expanding cities, the increasing trend of SUHI in shrinking cities is weak and slow. Thus, we believe that the SUHI effect is also alleviated with population shrinkage. But the specific driving mechanism behind it remains to be further explored. In general, this study is helpful to understand the impact of population shrinkage more comprehensively and take corresponding measures in time.

Declaration of Competing Interest

The authors declare that they have no known competing financial interests or personal relationships that could have appeared to influence the work reported in this paper.

References

Chakraborty, T., & Lee, X. (2019). A simplified urban-extent algorithm to characterize surface urban heat islands on a global scale and examine vegetation control on their spatiotemporal variability. *International Journal of Applied Earth Observation and Geoinformation, 74*, 269–280.

Chen, S., & Wang, T. (2009). Comparison analyses of interval method and mean-standard deviation method used to delimitate urban heat island. *Journal of Geo-Information Science, 11*, 145–150.

Cheng, Z., Yang, X., Sun, C., & Xu, Y. (2016). The trend of summer urban heat island effect and its relationship with urban development in Chengdu. *Climate Change Research, 12*, 322–331.

Danko, I. J. J., & Hanink, D. M. (2018). Beyond the obvious: A comparison of some demographic changes across selected shrinking and growing cities in the United States from 1990 to 2010. *Population, Space and Place, 24*, e2136.

Döringer, S., Uchiyama, Y., Penker, M., & Kohsaka, R. (2020). A meta-analysis of shrinking cities in Europe and Japan. Towards an integrative research agenda. *European Planning Studies, 28*, 1693–1712.

Emmanuel, R., & Krüger, E. (2012). Urban heat island and its impact on climate change resilience in a shrinking city: The case of Glasgow, UK. *Building and Environment, 53*, 137–149.

Friedl, M., & Sulla-Menashe, D. (2019). *MCD12Q1 MODIS/terra+aqua land cover type yearly L3 global 500m SIN grid V006*. N.E.L.P. DAAC.

Gao, S. (2015). *A review of researches on shrinking cities* (pp. 44–49). Urban Planning Forum.

Gu, D., Newman, G., Kim, J. H., Park, Y., & Lee, J. (2019). Neighborhood decline and mixed land uses: Mitigating housing abandonment in shrinking cities. *Land Use Policy, 83*, 505–511.

He, S. Y., Lee, J., Zhou, T., & Wu, D. (2017). Shrinking cities and resource-based economy: The economic restructuring in China's mining cities. *Cities, 60*, 75–83.

Hou, T. (2020). *Analysis of thermal environment changes in typical shrinking cities*. Harbin Normal University.

Imhoff, M. L., Zhang, P., Wolfe, R. E., & Bounoua, L. (2010). Remote sensing of the urban heat island effect across biomes in the continental USA. *Remote Sensing of Environment, 114*, 504–513.

Liu, G., Xie, F., Hong, J., & Chen, C. (2019). Urban shrinkage in China based on the data of population and economy. *Economic Geography, 39*, 50–57.

Long, Y., Wu, K., & Wang, J. (2015). Shrinking cities in China. *Modern Urban Research*, 14–19.

Martinez-Fernandez, C., Weyman, T., Fol, S., Audirac, I., Cunningham-Sabot, E., Wiechmann, T., & Yahagi, H. (2016). Shrinking cities in Australia, Japan, Europe and the USA: From a global process to local policy responses. *Progress in Planning, 105*, 1–48.

Meng, X., & Long, Y. (2022). Shrinking cities in China: Evidence from the latest two population censuses 2010-2020. *Environment and Planning A, 54*, 449–453.

Murdoch, I. I. I. J. (2018). Specialized vs. diversified: The role of neighborhood economies in shrinking cities. *Cities, 75*, 30–37.

Pan, M., Lan, S., Zhu, L., Liu, S., Zhang, X., & Xiu, X. (2020). Influence of landscape pattern types on heat island effect over central Fuzhou City. *China Environmental Science, 40*, 2635–2646.

Peng, S., Piao, S., Ciais, P., Friedlingstein, P., Ottle, C., Bréon, F.-M., Nan, H., Zhou, L., & Myneni, R. B. (2012). Surface urban heat island across 419 global big cities. *Environmental Science & Technology, 46*, 696–703.

Pichierri, M., Bonafoni, S., & Biondi, R. (2012). Satellite air temperature estimation for monitoring the canopy layer heat island of Milan. *Remote Sensing of Environment, 127*, 130–138.

Qiao, Z., & Tian, G. (2014). Spatiotemporal diversity and regionalization of the urban thermal environment in Beijing. *National Remote Sensing Bulletin, 18*, 715–734.

Schetke, S., & Haase, D. (2008). Multi-criteria assessment of socio-environmental aspects in shrinking cities. Experiences from eastern Germany. *Environmental Impact Assessment Review, 28*, 483–503.

Sun, W., & Li, H. (2013). Quantifying location condition of resources-exhausted cities in China. *Acta Geographica Sinica, 68*, 199–208.

Sun, Y., Gao, C., Li, J., Wang, R., & Liu, J. (2019). Evaluating urban heat island intensity and its associated determinants of towns and cities continuum in the Yangtze River Delta Urban Agglomerations. *Sustainable Cities and Society, 50*, Article 101659.

Sun, Y., Wang, R., Guo, Q., & Gao, C. (2021). Estimation of the urban heat island intensity change and its relationships with driving factors across China based on the human settlement scale. *Environmental Science, 42*, 501–512.

Venter Zander, S., Chakraborty, T., & Lee, X. (2021). Crowdsourced air temperatures contrast satellite measures of the urban heat island and its mechanisms. *Science Advances, 7*, eabb9569.

Wan, Z., Hook, S., & Hulley, G. (2015). *MOD11A1 MODIS/terra land surface temperature/emissivity daily L3 global 1km SIN grid V006*. N.E.L.P. DAAC.

Wang, Q. (2020). *Report on the work of Hegang Municipal People's Government in 2020*. http://www.hegang.gov.cn/szf/szf_zfgzbg/2020/04/26779.htm.

Wiechmann, T. (2008). Errors expected — aligning urban strategy with demographic uncertainty in shrinking cities†. *International Planning Studies, 13*, 431–446.

Wiechmann, T., & Pallagst, K. M. (2012). Urban shrinkage in Germany and the USA: A comparison of transformation patterns and local strategies. *International Journal of Urban and Regional Research, 36*, 261–280.

Wu, K. (2019). Cognitive misunderstanding and spatial planning response of city shrinkage. *Beijing Planning Review, 33*, 4–11.

Yang, Y., Wu, J., Wang, Y., Huang, Q., & He, C. (2021). Quantifying spatiotemporal patterns of shrinking cities in urbanizing China: A novel approach based on time-series nighttime light data. *Cities, 118*, Article 103346.

Yao, R., Wang, L., Huang, X., Niu, Z., Liu, F., & Wang, Q. (2017). Temporal trends of surface urban heat islands and associated determinants in major Chinese cities. *Science of The Total Environment, 609*, 742–754.

Zeng, X., & Duan, C. (2018). Performance evaluation and differential analysis on green transformation of coal resource-exhausted cities in China. *China Population, Resources and Environment, 28*, 127–135.

Zhan, W., Ju, W., Hai, S., Ferguson, G., Quan, J., Tang, C., Guo, Z., & Kong, F. (2014). Satellite-derived Subsurface Urban Heat Island. *Environmental Science & Technology, 48*, 12134–12140.

Zhang, S., Wang, C., Wang, J., Yao, S., Zhang, F., Yin, G., & Xu, X. (2020). On the comprehensive measurement of urban shrink in China and its spatio-temporal differentiation. *China Population, Resources and Environment, 30*, 72–82.

Zhou, D., Xiao, J., Bonafoni, S., Berger, C., Deilami, K., Zhou, Y., … Sobrino, J. A. (2019). Satellite remote sensing of surface urban heat islands: Progress, challenges, and perspectives. *Remote Sensing, 11*, 48.

Zhou, D., Zhao, S., Liu, S., Zhang, L., & Zhu, C. (2014). Surface urban heat island in China's 32 major cities: Spatial patterns and drivers. *Remote Sensing of Environment, 152*, 51–61.

Zhou, D., Zhao, S., Zhang, L., Sun, G., & Liu, Y. (2015). The footprint of urban heat island effect in China. *Scientific Reports, 5*, 11160.

Zhu, G., & Li, Y. (2015). Types and changes of Chinese climate zones from 1961 to 2013 based on Köppen climate classification. *Arid Land Geography, 38*, 1121–1132.

Zhu, P., Xiao, H., & Tian, H. (2010). Study on heat island effect based on GIS-ESDA. *Journal of Natural Disasters, 19*, 6–14.